Separation Science and Technology
Publication details, including instructions for authors and subscription information:
http://www.informaworld.com/smpp/title~content=t713708471

Impulse Response Analysis for Adsorption of Ethyl Acetate on Activated Carbon in Supercritical Carbon Dioxide

Motonobu Goto[a]; Masaki Sato[a]; Satoshi Kawajiri[a]; Tsutomu Hirose[a]
[a] DEPARTMENT OF APPLIED CHEMISTRY, KUMAMOTO UNIVERSITY, KUMAMOTO, JAPAN

To cite this Article Goto, Motonobu , Sato, Masaki , Kawajiri, Satoshi and Hirose, Tsutomu(1996) 'Impulse Response Analysis for Adsorption of Ethyl Acetate on Activated Carbon in Supercritical Carbon Dioxide', Separation Science and Technology, 31: 12, 1649 — 1661
To link to this Article: DOI: 10.1080/01496399608000716
URL: http://dx.doi.org/10.1080/01496399608000716

SEPARATION SCIENCE AND TECHNOLOGY, **31**(12), pp. 1649–1661, 1996

Impulse Response Analysis for Adsorption of Ethyl Acetate on Activated Carbon in Supercritical Carbon Dioxide

MOTONOBU GOTO,* MASAKI SATO, SATOSHI KAWAJIRI, and TSUTOMU HIROSE
DEPARTMENT OF APPLIED CHEMISTRY
KUMAMOTO UNIVERSITY
KUMAMOTO 860, JAPAN
FAX: +81-96-342-3679
E-MAIL: mgoto@gpo.kumamoto-u.ac.jp

ABSTRACT

Adsorption equilibria and mass transport properties for ethyl acetate on activated carbon have been evaluated in the presence of supercritical carbon dioxide by means of the impulse response technique. A two-column system, one for dissolving solute and one for adsorption, was used to evaluate the phenomena purely in the adsorption column. The adsorption equilibrium constant was larger for higher temperature and lower pressure. The apparent heat of adsorption calculated from the temperature dependence of the adsorption equilibrium constant was 30–40 kJ/mol. The intraparticle effective diffusivity was larger for higher temperature and lower pressure. The Peclet number that relates to the axial dispersion coefficient was 0.08–0.39. These estimated parameters are in good agreement with those obtained from desorption measurements reported in the literature.

Key Words. Adsorption; Supercritical fluid; Ethyl acetate; Carbon dioxide; Equilibria; Mass transfer

* To whom correspondence should be addressed.

INTRODUCTION

Supercritical fluids have received widespread attention in various fields. Important applications are in separation, extraction, and purification processes. In these processes solid materials are often involved as raw materials for extraction or as separating agents such as adsorbent or packing materials. Adsorption phenomena at the fluid–solid interface within a porous solid matrix may play an important roll in these processes.

Regeneration of adsorbents or desorption with supercritical fluids has been studied (1–9). Supercritical fluid extraction of organic contaminants from soil is an important environmental application of supercritical technology (10). Among these works, the ethyl acetate/activated carbon system was often employed because of its practical importance in petrochemical and polymer industries.

Extraction or desorption has been modeled to analyze the underlying phenomena including equilibrium, kinetic, and mass transport processes. Tan and Liou (6) analyzed the desorption behavior by an irreversible, first-order kinetic model. Recasens et al. (5) developed a general mathematical model including axial dispersion, external and intraparticle mass transfer, and nonlinear adsorption–desorption kinetics. A simplified local equilibrium model with a linear driving force model was used to explain the desorption data of Tan and Liou (6). Srinivasan et al. (2) applied a first-order, reversible adsorption model to the desorption of ethyl acetate from activated carbon. They concluded that the kinetics of desorption, as well as intraparticle mass transfer, influences the overall rate of desorption.

Erkey and Akgerman (11) applied chromatography theory to analyze the adsorption process of naphthalene on alumina where moment analysis of the dynamic tracer response was used. They evaluated adsorption equilibria and mass transport processes.

In this paper the adsorption–desorption process of ethyl acetate on activated carbon is evaluated by the tracer response technique. The results are compared with those obtained from a desorption experiment (2). The tracer response technique may be easier than the desorption experiment because a supercritical chromatograph is available. Moreover, the initial behavior of the extraction measurement is difficult to describe by a simple model. It may be worthwhile to obtain information for the desorption process by the response technique.

EXPERIMENTAL

Impulse response measurements were carried out with the supercritical fluid chromatograph Super-200 (Jasco) with minor modification. A sche-

matic diagram of the experimental setup is shown in Fig. 1. Carbon dioxide from a cylinder with a siphon attachment is passed through a cooled water bath and compressed to the operating pressure by a pump (880-PU, Jasco). The compressed fluid is passed through an injector and two columns, one (called the "pre-column") for dissolving solute and the other (called the "adsorption column") for adsorption analysis. The injector and columns are placed in a constant-temperature bath. The effluent from one of these columns is passed through a UV-visible spectrophotometer (870-UV, Jasco) to measure the concentration of solute in the supercritical carbon dioxide. The fluid is then expanded to ambient pressure through a back-pressure regulator (880–81, Jasco) placed after the detector.

The pre-column is 12.5 mm long and of 10 mm i.d., and the adsorption column is 50 mm long and of 7.6 mm i.d. Activated carbon (Charcoal Activated, Nacalei Tesque) was used as the solid phase. The activated carbon particles were crashed, sieved, washed, and dried. The activated carbon was packed in both pre- and adsorption columns. The adsorbate was ethyl acetate (Wako Chem. Ind.). The specifications of the adsorption column are given in Table 1.

Ethyl acetate (10 μL) was injected, and the response was monitored at the exit of the pre-column and at the exit of the adsorption column. The response curve at the exit of the pre-column was regarded as the input

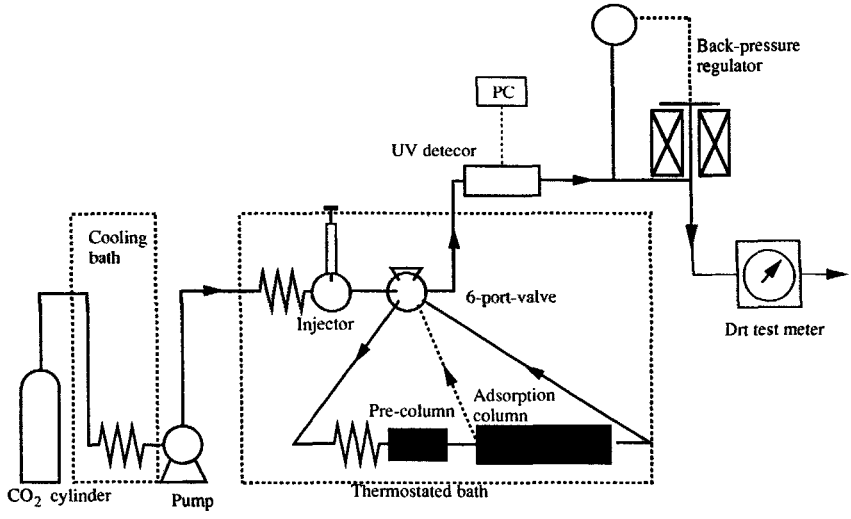

FIG. 1 Experimental setup.

TABLE 1
Properties of the Adsorption Bed

Bed length	50.0 mm
Bed radius	3.8 mm
Bed porosity, α	0.40
Particle radius	0.385 mm
Particle porosity, β	0.66
Particle density, ρ_p	581 kg/m^3

of the adsorption column. Thus, the difference in response curves at the exit of the pre-column and at the exit of the adsorption column may involve purely adsorption and mass transport phenomena in the adsorption column. In the other word, undesirable phenomena at the injector can be reduced. The operation temperatures were 308, 313, and 323 K, and the operation pressures were 8.22, 10.9, and 16.6 MPa.

THEORETICAL DEVELOPMENT

The impulse response in a packed column is governed by a system of coupled partial differential equations that includes axial dispersion, external fluid-particle mass transfer, and intraparticle diffusion. Adsorption isotherm is assumed to be linear. Mass conservation equations for the solute in the void region, in the pores, and on the particles are, respectively,

$$\frac{\partial C}{\partial t} + v\frac{\partial C}{\partial z} = E\frac{\partial^2 C}{\partial z^2} - \frac{3(1-\alpha)}{\alpha r_0}k_f[C - (C_i)_{r=r_0}] \tag{1}$$

$$\beta\frac{\partial C_i}{\partial t} = D_e\frac{1}{r^2}\frac{\partial}{\partial r}\left(r^2\frac{\partial C_i}{\partial r}\right) - \frac{\partial C_s}{\partial t} \tag{2}$$

$$\frac{\partial C_s}{\partial t} = k_a\left(C_i - \frac{C_s}{K_A}\right) \tag{3}$$

The solution of these equations in the Laplace domain leads to the moment expressions (12). The first absolute and the second central moments of the response curve for the system are, respectively,

$$\mu_1' = \frac{z}{v}(1 + \delta_0) \tag{4}$$

$$\mu_2 = \frac{2z}{v}\left[\delta_1 + \frac{E}{v^2}(1 + \delta_0)^2\right] \tag{5}$$

where

$$\delta_0 = \frac{1 - \alpha}{\alpha}(\beta + K_A) \tag{6}$$

$$\delta_1 = \frac{1 - \alpha}{\alpha}\left[\frac{K_A^2}{k_a} + (\beta + K_A)^2\left(\frac{1}{5D_e} + \frac{1}{k_f r_0}\right)\frac{r_0^2}{3}\right] \tag{7}$$

The first absolute moment, μ_1', characterizes the position of the center of gravity of the response peak, whereas the second central moment, μ_2, characterizes the width of the peak.

In the analysis of the experimental data, the intrinsic adsorption rate, k_a, was assumed to be infinitely large because the adsorption rate may be much larger than the mass transfer rate in the chromatographic process. The validity of this assumption is shown later. The external fluid-particle mass transfer coefficient, k_f, was estimated by the Wakao–Kaguei correlation (13).

The first and second moments of the experimental response curve are calculated by

$$\mu_1' = \int_0^\infty Ct\,dt \Big/ \int_0^\infty C\,dt \tag{8}$$

$$\mu_2 = \int_0^\infty C(t - \mu_1')^2\,dt \Big/ \int_0^\infty C\,dt \tag{9}$$

RESULTS AND DISCUSSION

Adsorption Equilibrium Constant

The linearity of the adsorption equilibria was checked by injecting various amounts of the solute. The response curves at the exit of the adsorption column are shown in Fig. 2. Since the peak position was not influenced by the amount of sample, the adsorption equilibria could be regarded as a linear isotherm as assumed in Eq. (3). Thus, the moment analysis using Eqs. (4)–(7) can be applied.

Equation (4) indicates that a plot of μ_1' versus z/v gives a straight line through the origin. The adsorption equilibrium constant, K_A, can be obtained from the slope of the line by the following procedure. Since the input signal into the adsorption column is not a delta function or a square pulse, the response curves at the exit and inlet of the adsorption column must be used to evaluate the behavior inside the adsorption column. Addi-

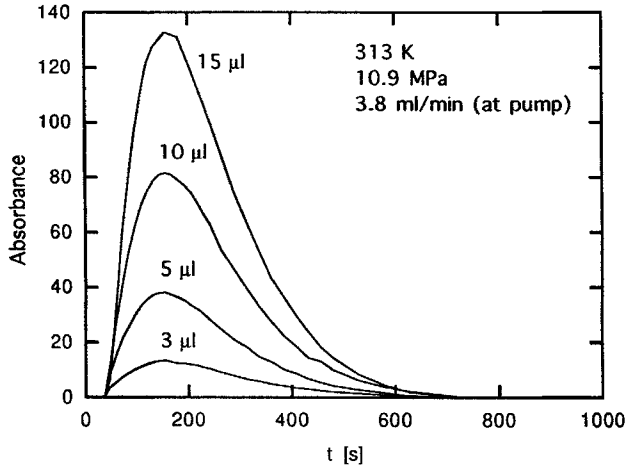

FIG. 2 Effect of sample amount on the response curve.

tive properties of the moments enable the behavior in the column to be evaluated by subtracting the moments at the inlet of the column from the moments at the exit of the column. The first moment $\Delta\mu_1'$, that is, the moment at the exit of the adsorption column, μ_1'(outlet), subtracted from the one at the inlet of the adsorption column, μ_1'(inlet), measured at various flow rates, was plotted against z/v. The plot at 10.9 MPa is shown in Fig. 3. Experimental data lay on a single straight line through the origin with a correlation coefficient larger than 0.997.

The adsorption equilibrium constant, K_A, evaluated from the slopes of the straight lines, is shown in a van't Hoff plot in Fig. 4. The adsorption equilibrium constant increased with an increase in temperature and a decrease in pressure. These temperature and pressure dependences are common in the retrograde region and are consistent with thermodynamic analysis (14), although they are opposite to adsorption behavior under ambient conditions. The results obtained by Srinivasan et al. (2) from desorption measurement are compared with ours in Fig. 4. Although the activated carbon and experimental method are different in Ref. 2 from our work, the adsorption equilibrium constants agree well. The temperature dependence of the adsorption equilibrium constant in this work was larger than that for Srinivasan et al. (2).

The apparent heat of adsorption, ΔH_{app}, was estimated from the slope the best fit line. Our obtained values of ΔH_{app} are compared with the results of Srinivasan et al. (2) in Table 2. The apparent heat of adsorption

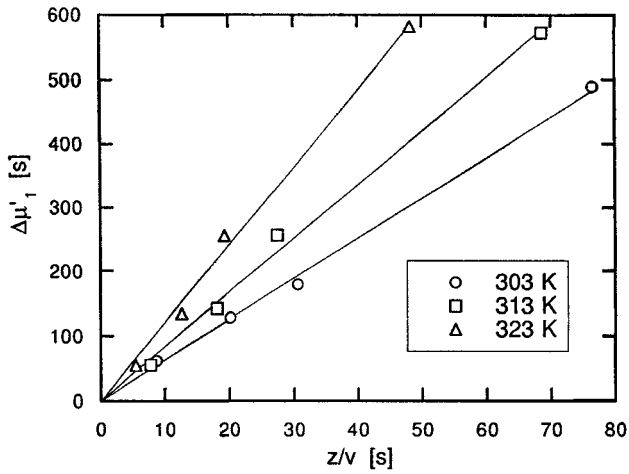

FIG. 3 Plots of first absolute moment at 10.9 MPa.

obtained by Srinivasan et al. (2) was 13–20 kJ/mol. Recasens et al. (5) obtained 50 kJ/mol for a different type of activated carbon. Macnaughton and Foster (9) obtained 31.4 kJ/mol for DDT on activated carbon. The value obtained in this work, 30–40 kJ/mol, is in good agreement with those reported in the literature. The slight differences could be due to the different activated carbons used.

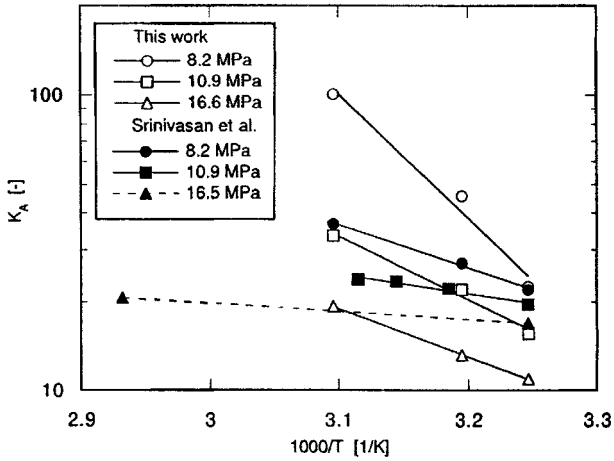

FIG. 4 Adsorption equilibrium constant in van't Hoff plots.

TABLE 2
Apparent Heat of Adsorption

	ΔH_{app} (kJ/mol)	
P (MPa)	This work	Srinivasan et al. (2)
8.22	101	19.6
10.9	41.1	13.4
16.6	31.1	(5.24)[a]

[a] Calculated from two estimates. They may have large errors.

The capacity factor, k, which is conventionally used in chromatography, is related to adsorption equilibrium constant K_A by

$$k = \frac{(1 - \alpha)K_A}{\alpha + (1 - \alpha)\beta} \tag{10}$$

The capacity factor plotted in ln k vs ln ρ gives a straight line independent of the pressure (3, 11). As shown in Fig. 5, the capacity factor agrees well with those of Srinivasan et al. (3). The capacity factor lies almost on a straight line for lower density. At higher density or higher pressure, the values tended to deviate from the straight line.

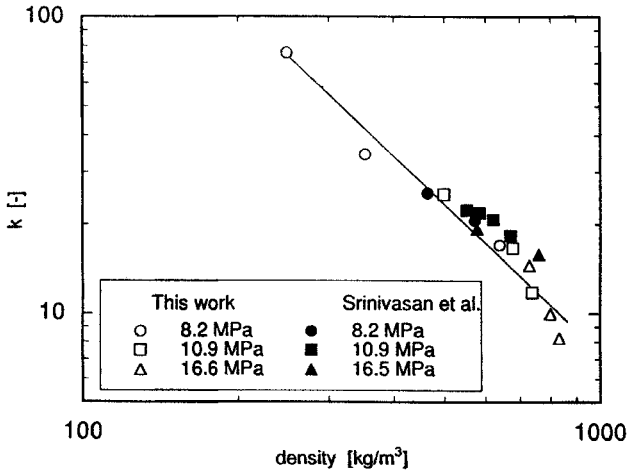

FIG. 5 Variation of capacity factor with density.

Mass Transport Processes

Each mass transport step can be estimated by the second moment due to the additive properties. The second moment, $\Delta\mu_2 = \mu_2(\text{outlet}) - \mu_2(\text{inlet})$, was calculated as in the case of first moment. Equations (4) and (5) were rearranged to

$$\frac{\Delta\mu_2}{2\Delta\mu_1'} = \frac{\delta_1}{1 + \delta_0} + (1 + \delta_0)\frac{E}{v^2} \tag{11}$$

Since E/v can be considered to be constant at low Reynolds numbers in packed beds, a plot of left-hand side of Eq. (11) against $1/v$ may give a straight line with an intercept of $\delta_1/(1 + \delta_0)$ and a slope of $(1 + \delta_0)E/v$. Figure 6 shows the second moment plot at 10.9 MPa. The experimental data lie on a straight line with the correlation coefficient larger than 0.98. Consequently, the intraparticle effective diffusivity, D_e, is calculated from the intercept, and the axial dispersion coefficient, E, is calculated from the slope.

The results are summarized in Table 3. The ratio of the intraparticle effective diffusivity to the molecular diffusivity, D_e/D_{AB}, is shown in the seventh column. The Peclet number, $\text{Pe} = 2vr_0/E$, is calculated from axial dispersion coefficient E. The binary diffusivity D_{AB} was estimated by the method of Takahashi (15), and the external mass transfer coefficient by the Wakao–Kaguei correlation (13).

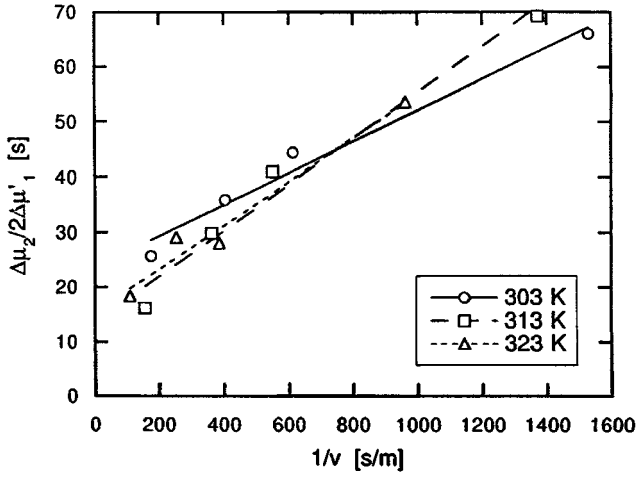

FIG. 6 Plots of second central moment at 10.9 MPa.

TABLE 3
Mass Transport Parameters

P (MPa)	T (K)	ρ (kg/m^3)	$\mu \times 10^6$ (kg/m·s)	$D_{AB} \times 10^9$ (m^2/s)	$D_e \times 10^9$ (m^2/s)	D_e/D_{AB} (—)	Pe (—)
8.22	308	610.1	30.5	47.0	15.4	0.328	0.390
8.22	313	299.5	23.3	53.0	42.9	0.810	0.132
10.9	308	738.1	57.2	17.0	10.1	0.593	0.171
10.9	313	678.0	47.6	24.5	22.4	0.913	0.158
10.9	323	498.9	31.1	29.6	38.8	1.310	0.236
16.6	308	833.4	73.2	8.95	9.89	1.105	0.080
16.6	313	800.8	67.6	9.20	16.0	1.738	0.099
16.6	323	729.5	56.3	14.6	24.1	1.652	0.136

The intraparticle effective diffusivity was larger for higher temperature and lower pressure. The ratio D_e/D_{AB}, which was expected less than unity due to tortuosity, was from 0.3 to 1.7. Since the estimated binary diffusivity has a large error as well as an experimental error, the ratio D_e/D_{AB} may not be informative. The intraparticle effective diffusivity D_e, calculated from Srinivasan et al. (2), was 7.3×10^{-9} m^2/s at 10.9 MPa and 313 K, and is about one-third of that in this work.

The Peclet number was from 0.08 to 0.39 and was larger for lower temperature and lower pressure. The Peclet numbers obtained by Erkey and Akgerman (11) ranged from 0.058 to 0.25 and were in good agreement with those in this work. As mentioned by Erkey and Akgerman (11), the dependence of Pe on pressure suggests that the dispersion process is controlled by convection and not by molecular diffusion.

The contribution of each rate process on the second central moment, that is, peak broadening, was evaluated by using estimated parameters. Figure 7 shows the relative contribution of adsorption kinetics, intraparticle diffusion, external mass transfer, and axial dispersion to the second central moment, Eqs (5)–(7), as a function of Reynolds number in this experimental region at 313 K and 10.9 MPa. Since the adsorption rate constant k_a could not be determined in this work, the parameter obtained by Srinivasan et al. (2) was used. The contribution of axial dispersion decreased with an increase in Re or in the flow rate, whereas the contribution of the other rate processes increased. The intraparticle diffusion resistance contributed enough for the parameter estimation, especially at higher flow rate. On the other hand, the contribution of adsorption rate k_a was small, indicating that evaluation of the adsorption rate constant from this experiment is not possible.

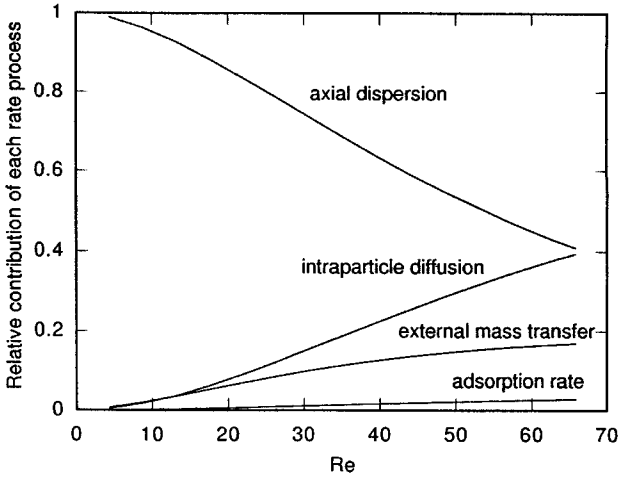

FIG. 7 Contribution of each rate process to peak broadening.

The evaluation of rate processes from the second central moment is usually more difficult than the evaluation of equilibria from the first moment, because the second central moment obtained from experimental measurement has a much larger error than the first moment. Since a two-column system was used to subtract the effect of injection irregularity, the moment calculated has an even larger error. Although the response measurement with a single column may give an analysis with less error than the two-column system, the irregularity at the injector port, including slow dissolving of solute into the fluid and the unknown shape of the impulse, cannot be removed.

Fine-tuning the experimental setup might give a more reliable analysis. Since the parameters obtained in this work almost agree with those obtained from desorption measurement by Srinivasan et al. (2), the parameters obtained by the impulse response method can be used for the design and analysis of the desorption process.

CONCLUSION

The impulse response technique has been applied for the adsorption system in the presence of a supercritical fluid. In order to reduce the undesired effect at the injector, a two-column system was employed. The adsorption equilibrium constant, intraparticle effective diffusivity, and axial dispersion coefficient were evaluated by analyzing the moments of

the response curve. The parameters obtained agreed well with those obtained from desorption measurement (2). This technique may be applicable to more complicated systems including the adsorption/desorption process, partitioning, and reactions.

SYMBOLS

C	concentration in fluid phase (mol/m^3)
C_i	concentration in pore space (mol/m^3)
C_s	concentration in solid phase (mol/m^3)
E	axial dispersion coefficient (m^2/s)
D_{AB}	binary diffusivity (m^2/s)
D_e	intraparticle effective diffusivity (m^2/s)
K_A	adsorption equilibrium constant
k	capacity factor
k_a	adsorption rate constant (1/s)
k_f	fluid to particle mass transfer coefficient (m/s)
Pe	Peclet number, $2r_0v/E$
r	radial coordinate
r_0	particle radius (m)
Re	Reynolds number, $2r_0v\rho/\mu$
t	time (s)
u	superficial fluid velocity (m/s)
v	interstitial fluid velocity (m/s)
z	bed height (m)

Greek Letters

α	bed void fraction
β	particle voidage
μ	fluid viscosity (kg/m·s)
μ_1'	first absolute moment (s)
μ_2	second central moment (s^2)
ρ	fluid density (kg/m^3)

REFERENCES

1. R. G. Kander and M. E. Paulaitis, "The Adsorption of Phenol from Dense Carbon Dioxide onto Activated Carbon," in *Chemical Engineering at Supercritical Fluid Conditions* (M. E. Paulaitis, J. M. L. Penninger, R. D. Gray, and P. Davidson, Eds.), Ann Arbor Science, Ann Arbor, Michigan, 1983, pp. 461–476.
2. M. P. Srinivasan, J. M. Smith, and B. J. McCoy, "Supercritical Fluid Desorption from Activated Carbon," *Chem. Eng. Sci.*, *45*(7), 1885–1895 (1990).

3. M. P. Srinivasan and B. J. McCoy, "Partial Molar Volumes of Ethyl Acetate from Supercritical CO_2 Desorption Data," *J. Supercritical Fluids*, *4*, 69–71 (1991).
4. M. P. Srinivasan, J. M. Smith, and B. J. McCoy, "Ethyl Acetate Desorption from Activated Carbon with Supercritical Carbon Dioxide: Effect of Initial Loading," *Chem. Eng. Sci.*, *46*(1), 371–374 (1991).
5. F. Recasens, B. J. McCoy, and J. M. Smith, "Desorption Processes: Supercritical Fluid Regeneration of Activated Carbon," *AIChE J.*, *35*, 951–958 (1989).
6. C.-S. Tan and D.-C. Liou, "Desorption of Ethyl Acetate from Activated Carbon by Supercritical Carbon Dioxide," *Ind. Eng. Chem. Res.*, *27*, 988–991 (1988).
7. C.-S. Tan and D.-C. Liou, "Supercritical Regeneration of Activated Carbon Loaded with Benzene and Toluene," *Ibid.*, *28*, 1222–1226 (1989).
8. G. Madras, C. Erkey, and A. Akgerman, "Supercritical Fluid Regeneration of Activated Carbon Loaded with Heavy Molecular Weight Organics," *Ibid.*, *32*, 1163–1168 (1993).
9. S. J. Macnaughton and N. R. Foster, "Supercritical Adsorption and Desorption Behavior of DDT on Activated Carbon Using Carbon Dioxide," *Ibid.*, *34*, 275–282 (1995).
10. A. Akgerman, C. Erkey, and S. M. Ghoreishi, "Supercritical Extraction of Hexachlorobenzene from Soil," *Ibid.*, *31*, 333–339 (1992).
11. C. Erkey and A. Akgerman, "Chromatography Theory: Application to Supercritical Fluid Extraction," *AIChE J.*, *36*(11), 1715–1721 (1990).
12. M. Suzuki, *Adsorption Engineering*, Kodansha and Elsevier, 1990, pp. 125–150.
13. N. Wakao and S. Kaguei, *Heat and Mass Transfer in Packed Beds*, Gordon & Breach, New York, 1985.
14. F. D. Kelly and E. H. Chimowitz, "Near-Critical Phenomena and Resolution in Supercritical Fluid Chromatography," *AIChE J.*, *36*, 1163–1175 (1990).
15. R. C. Reid, J. M. Prausnitz, and B. E. Poling, *The Properties of Gases & Liquids*, 4th ed., McGraw-Hill, New York, 1987.

Received by editor September 13, 1995